Calcif Tissue Int (1996) 58:423–428

Calcified Tissue International

Bicarbonate Dependence of Ion Current in Damaged Bone

A. Rubinacci,[1] A. De Ponti,[2] A. Shipley,[3] M. Samaja,[2] E. Karplus,[3] L. F. Jaffe[3]

[1]Istituto Scientifico H San Raffaele, via Olgettina 60, 20132 Milano, Italy
[2]Università degli Studi di Milano, Milano, Italy
[3]Marine Biological Laboratory, Woods Hole, Massachusetts, USA

Received: 28 December 1994 / Accepted: 1 December 1995

Abstract. The aim of this work was to characterize the ion current that enters mouse metatarsal bones following damage to the cortex. We assessed both the spatial distribution of this current and its dependence on the presence of bicarbonate in the medium. We used a voltage-sensitive probe system vibrating in two dimensions and recorded the signal as function of the position of the probe with respect to the site of damage and of ion substitutions in the medium. When the cortex was damaged (50 μm cylindrical hole penetrating into the marrow cavity), we recorded a steady state net inward electrical current directed toward the site of damage. In nonbicarbonate media, the density of the current was maximal near the center of the hole and ranged from 6 to 18 $\mu A/cm^2$. As the probe was moved off the center of the hole, measured current density decreased in a manner consistent with the hypothesis that the source of the inward current is localized to the hole. After changing bicarbonate concentration in the medium from 0 to 42 mM, the current density nearly doubled, then decayed back to its original level exponentially over 35 minutes. When the diaphysis of living bone was left intact the current density was close to background level either in the presence or absence of bicarbonate in the medium. Damaged dead bone did not drive any current higher than background level. We conclude that the vibrating probe technique is a powerful tool to characterize ion currents in injured bone, helping to understand the physiology of bone-plasma interface and the bone healing processes. The current density transiently doubled upon addition of bicarbonate, indicating that this ion may carry the electrical current in damaged bone, probably by pump-leak mechanisms operating at the bone-plasma interface.

Key words: Bone — Fracture — Ion currents — Bicarbonate.

The healing process of damaged bones involves an inward ion current directed toward the site of damage [1]. This phenomenon was assessed by a one-dimension vibrating probe technique [1] optimized to measure small ion currents emerging from tissues or cells [2]. The ion current that follows damage to the cortex of mouse metatarsal is the result of a decaying (flexure) and a steady state persistent (plateau) current [1]. The former is associated with deformation of bone tissue and likely originates from streaming potentials. The latter is associated with viability of bone cells and originates from pump-leak mechanisms at the bone-plasma interface [1].

Measurements of plateau current changes following ion substitution showed that chloride and, to a less extent, sodium, magnesium, and calcium may act as current carriers and are exchanged at the bone-plasma interface [1]. Several features point to bicarbonate as an additional ion species involved in the above mechanisms: (1) the skeleton is a major storage area of bicarbonate [3]; (2) bone bicarbonate is rapidly available to buffer acute acid load in plasma [4], and (3) bicarbonate transport is associated with that of chloride [5], that is a recognized current carrier in bone [1].

The aim of this study was to characterize by novel methods the plateau current at the damaged site of bone cortex and to determine if the density of this current depends on the presence of bicarbonate. For these purposes, we used a two-dimensional vibrating probe [6] that provides several advantages over a one-dimensional vibrating probe. Our results indicate that stable inward currents enter the site of damage along specific pathways, and that the intensity of these currents depends on the presence of bicarbonate in the medium.

Materials and Methods

Materials

The ion composition of the media (Table 1) resembles the BGJb medium, extensively used for bone culture [7, 8]. Media were equilibrated in air before bicarbonate addition to assure adequate pO_2. Reagents were provided by Sigma (St. Louis, MO, USA) and were of the highest available purity. Weanling Swiss mice (Nossan, Italy) were anesthetized with CO_2 and killed by cervical dislocation. The back limbs were amputated at the distal tibia epiphysis and immersed in the appropriate incubation medium. The second or third metatarsal bones were dissected intact from the digit with care to avoid damage to the bone surface. All manipulations were carried out on samples immersed in the medium at room temperature with an M3 surgical microscope (Wild, Zurich, Switzerland). After the bone was freed of soft tissue ensheathments, a 50-μm-diameter hole penetrating into the marrow cavity was made with a thin needle through the diaphyseal cortex.

Experimental Setup

All equipment (chamber, probe electrode, and microscope) was placed on a M-TS 23 antivibration platform (Newport, Fountain Valley, CA, USA). The bone was held at the bottom of a specifi-

Correspondence to: A. Rubinacci

Table 1. Composition of the media used in this study (mM)

Media	Medium		
	Bicarbonate	Sulfate	Isethionate
$NaHCO_3$	42	—	—
Na_2SO_4	—	21	—
Na isethionate	—	—	42
NaCl	75	75	75
Na_2HPO_4	0.8	0.8	0.8
NaH_2PO_4	0.2	0.2	0.2
KCl	5.4	5.4	5.4
Ca lactate	1.8	1.8	1.8
$MgSO_4$	0.4	0.4	0.4
Glucose	132	153	132
HEPES	10	10	10

pH and osmolarity were 7.33 ± 0.03 and 387 ± 7 mOsm, at a temperature of 36.9 ± 0.6°C (mean ± SD)

cally built Petri dish by gluing its ends with histoacrylic glue to two nylon holders (Fig. 1). The dish was filled with appropriate prewarmed (37°C) medium, and mineral light white oil was layered onto it. The dish was then immersed in an aluminum container over a Peltier heating chip kept at 37°C. Medium pH was monitored either by a PHM 83 pHmeter (Radiometer, Copenhagen, Denmark) placed in the chamber or by a $pH/pO_2/pCO_2$ automatic analyzer (Instrumentation Laboratory, Lexington, MA, USA) on aliquots taken during incubation. Osmolarity was measured by a Osmostat Os 6020 pressure osmometer (Damchi, Kyoto, Japan). Temperature was monitored by a T801 thermoprobe (Radiometer, Copenhagen, Denmark).

Data Acquisition

A BH Olympus microscope (Tokyo, Japan) was connected to a video camera (TK S200, JVC, Tokyo, Japan) and an RGB monitor (EUM1491A, Mitsubishi, Tokyo, Japan). The area that includes the vibrating probe electrode, the bone surface, and the upper section of the hole were viewed at 18.23 mm working distance by a D-achromat A4 ×4 lens (Olympus, Tokyo, Japan). Light was provided by optic fiber cables (Olympus), connected to a cold light source (Intralux 5000, Volpi, Zurich, Switzerland).

The two-dimensional vibrating probe system has been described in detail [6, 9]. Briefly, the reference electrode (stationary platinum black wire) was immersed in the medium. The probe was an insulated stainless-steel electrode (SS 300305A, Microprobe Inc., Clarksburg, MD) with a platinum black tip. The probe is vibrated between two positions along X and Y directions by means of a π-shaped linkage of three rectangular piezoelectric bimorphs to which sinusoidal signals are applied. The probe measures the electrical potential differences between the extremes of its excursion along the directions of vibration. The signal is amplified and transferred via an A-D converter (DAS8, Keithley Metrabyte, Taunton, MA) to a computer for data acquisition and storage. The software allows the recording of the probe position in the computer, analyzes the two orthogonal components of the measured signal, and expresses them by an average vector (PCVision Plus, Imaging Technology Inc., Bedford, MA) overlaid on the digitized image (RGB monitor) of the bone. Each vector represents density, direction, and sign of the current at the measurement point corresponding to the arrow head. The analog outputs of the system were also recorded on a four-channel chart recorder (BD101, Kipp & Zonen, Delft, Holland).

To calibrate the probe, 50 nA current was delivered into a medium (resistance ~100 Ω/cm) by a glass micropipette (1 × 90 mm, GD-1, Narishige, Tokyo, Japan) filled with 3M KCl and with a small-diameter tip, obtained by a micropipette puller (PB-7, Narishige, Tokyo, Japan). The current source was placed (3-D micromanipulator, M-152, Narishige) at two locations 150 μm away from the probe, in mutually orthogonal directions.

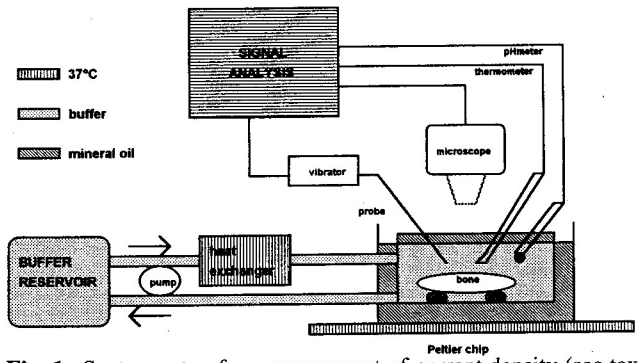

Fig. 1. System setup for measurement of current density (see text for detailed description).

Signals out of phase with the probe vibration (quadrature output) usually indicate the presence of artifacts, such as contact with the tissue under study [10]. Measurements were not considered if such signals were observed.

Typically, the vibrating probe was calibrated each day and a new probe electrode was used for each experiment. The background value was first measured by placing the probe far from the bone (>3 mm). The experiment was aborted for background values >0.5 $\mu A/cm^2$. Then, the probe was moved using a 3D micromanipulator (MO-203, Narishige, Tokyo, Japan) to 35–50 μm above the cortical hole to map the current densities in the surroundings of the hole. The actual current density was obtained by subtracting the background value to the reading thus correcting for electrode drifts. The obtained coefficient of variation when the location was kept constant was 7%.

The planes of vibration were the X plane normal to the longitudinal axis of the bone diaphysis and the Y plane parallel to the bone surface. Vectors along the X and Y planes and the video image of the bone itself were printed by a TX 1000 thermal color printer (Polaroid, Cambridge, MA).

Experimental Protocol

All bones (n = 19) were first studied for spatial distribution of current density near the site of damage. When stable background readings were obtained (5–10 minutes after making the hole), we scanned the area around the hole by moving the probe along the bone longitudinal axis. During scanning, we held the probe at a distance of 20–40 μm from the bone surface to minimize interferences [11]. We tested the vectors at five to eight positions near the hole along the bone longitudinal axis.

After testing the spatial distribution of current density, the probe was located at the point of maximal density, that was always found over the center of the hole, and held it in place to examine the effect of ion substitution. The point of maximal current density was recognized by the position where the vector entering the site of damage was longest. This position was automatically recorded by the software and by a marker in the video image to ensure that the probe electrode is positioned on the same location during the ion substitution experiments. The dish was repeatedly emptied and filled with prewarmed medium through inlet and outlet tubes, anaerobic connections, and a Mini-S840 peristaltic pump (PBI International, Milano, Italy). Bone was alternately incubated in the medium containing a bicarbonate substitute (sulfate or isethionate) and in the bicarbonate containing medium. For this typical experiment, sequence and timing were as follows: sulfate or isethionate medium (15 minutes), sulfate or isethionate (15 minutes), bicarbonate (35 minutes), sulfate or isethionate (15 minutes), bicarbonate (20 minutes), sulfate or isethionate (15 minutes). The total elapsed time for the experiments involving bicarbonate-containing medium was about 2 hours.

Bone was also alternately incubated in sulfate and isethionate media to test the effect of the medium exchange procedure on current density. Sequence and timing were as follows: sulfate (15 minutes), isethionate (15 minutes), sulfate (15 minutes), isethionate (15 minutes), sulfate (15 minutes). The total time elapsed for this experiment was about 80 minutes.

We performed three series of control experiments by measuring current density at the diaphysis of (1) intact living bone alternately incubated in sulfate, isethionate, and bicarbonate media (duration 60 minutes); (2) damaged dead bone as obtained after fixation in buffered formaldehyde solution and subsequent equilibration in medium for 3 days (duration 15 minutes); and (3) damaged living bone incubated in sulfate medium for 2 hours.

Statistics

Data are expressed as means ± SEM. To compare two groups, we used the two-tailed Student's t test for paired observations. Differences were considered significant for $P < 0.05$.

Results

Spatial Distribution of Current Vectors

In sulfate and isethionate medium, we always recorded a stable inward current after damage to the bone cortex. A typical map of the current vectors in the surroundings of the site of damage is shown in Figure 2A. The density of the current was maximal over the center of the hole, averaging 10.5 ± 3.4 $\mu A/cm^2$ (n = 12). The density of the current gradually decreased to background level (~0.5 $\mu A/cm^2$) as the probe was moved either along the longitudinal axis of the bone or away from the bone surface. The current vectors were constantly directed towards the center of the hole. The central vectors were perpendicular to the longitudinal axis of the diaphysis, and the peripheral ones were parallel to it.

At the diaphysis of intact living bone alternately incubated in isethionate, sulfate, and bicarbonate media (n = 2), we recorded current values close to the background level (Fig. 2B). At the damaged diaphysis of dead bone (n = 4) we did not measure any current higher than the background (Fig. 2C). When the current density was continuously monitored at the damaged diaphysis of three living bones incubated in sulfate medium, in no instance was it significantly different from the value taken at t = 0 minutes (Fig. 3).

We did not observe any significant difference of current value at the damaged diaphysis of living bone during sequential incubations in sulfate and isethionate media (Fig. 4).

Bicarbonate Dependence of Current Density

Blanks performed replacing sulfate with sulfate or isethionate with isethionate showed that current density changes due to media exchange (1.9 ± 1.3 $\mu A/cm^2$, n = 12) were not significant (Fig. 5). However, basal current density increased sharply when bicarbonate replaced sulfate or isethionate (n = 12, $P < 0.002$) (Fig. 5). Peak values were recorded as soon as the chamber was filled with bicarbonate (*early bicarbonate*). The current density then decayed in 10 of 12 bones to ~50% of peak value within 35 minutes (*late bicarbonate*). No decay was observed in two bones. The decay followed an exponential pattern of the 1st order with average rate constant at -0.090 ± 0.006 $minute^{-1}$ (n = 10). When sulfate or isethionate replaced bicarbonate (n = 11), the density returned to the value measured before bicarbonate, indicating that the effect of bicarbonate was reversible. As bicarbonate again replaced sulfate or isethionate, the same pattern as that described above was reproduced, but with lower peak values (n = 9, $P = 0.0001$).

Table 2 shows that pH, pO_2, pCO_2, HCO_3^-, and tot CO_2 were unchanged during the readings when bone was incubated in bicarbonate medium (elapsed time 35 minutes).

Discussion

Electrical Signals at the Damaged Diaphysis of Unstressed Living Bone

The two-dimensional vibrating probe system provides a useful tool to determine the distribution of ionic currents surrounding the site where physical damage is inferred to bones immersed in physiological media. This study stresses the occurrence of a steady ion current directed to the site of damaged diaphysis of unstressed living bone. No current was driven by the intact diaphysis of living bone or by the damaged diaphysis of dead bone, thus the recorded signal is strictly dependent on the viability of bone tissue and on the presence of bone damage. The peculiarity of the experimental setup allows one to map these currents, identify the position of maximal current density, and evaluate the effects of targeted ion substitution on current density. We observed that when bicarbonate replaces either sulfate or isethionate, current density increases sharply then decays to a plateau 50% lower than the peak value.

The vibrating probe system was previously used to measure steady ionic currents in several biological systems [9, 12]. This system allows sensitive evaluation of the asymmetric pattern of steady ionic current loops generated by ion pumps and leaks [13]. In the field of bone repair and growth, the vibrating probe system has helped to confirm the existence of endogenous electrical signals in bone by measuring a plateau current traversing the bone [1]. The occurrence of electrical signals on the surface of unstressed living bone was originally demonstrated by measuring bioelectrical potentials *in vivo* [14, 15], and their distribution pattern was described [16]. It was also shown that fractures quickly alter the distribution of bioelectrical potentials [14] and activate an endosteal battery that drives current into the injury [17]. However, no direct comparison can be made between *ex vivo* current density measurements and the *in vivo* bioelectrical potential measurements due to differences in materials and electrical measurement methods. For example, the electrical potential is affected by both resistance changes due to tissue drying and anatomical alterations of soft tissue ensheathments [18], and current pathways are therefore expected to be different from those *in vivo* [17].

In this study we essentially confirm the existence of the plateau ionic current component and thus the hypothesis that bone lesions quickly activate ionic currents entering the lesion itself [1]. These currents are driven by cells, being temperature dependent [1] and absent in dead bone.

The demonstration that bones drive ion currents is in agreement with the observations that bone is not in passive equilibration with the surrounding medium [19–24]. In fact, several lines of evidence suggest that bone fluid is compartmentalized and its ionic composition is different from the systemic extracellular fluid [25]. A cell layer, somehow constituting a bone membrane for ionic partition, should possess some kind of transporting epithelial cell-like properties [26]. Its location should be inside the bone, likely at

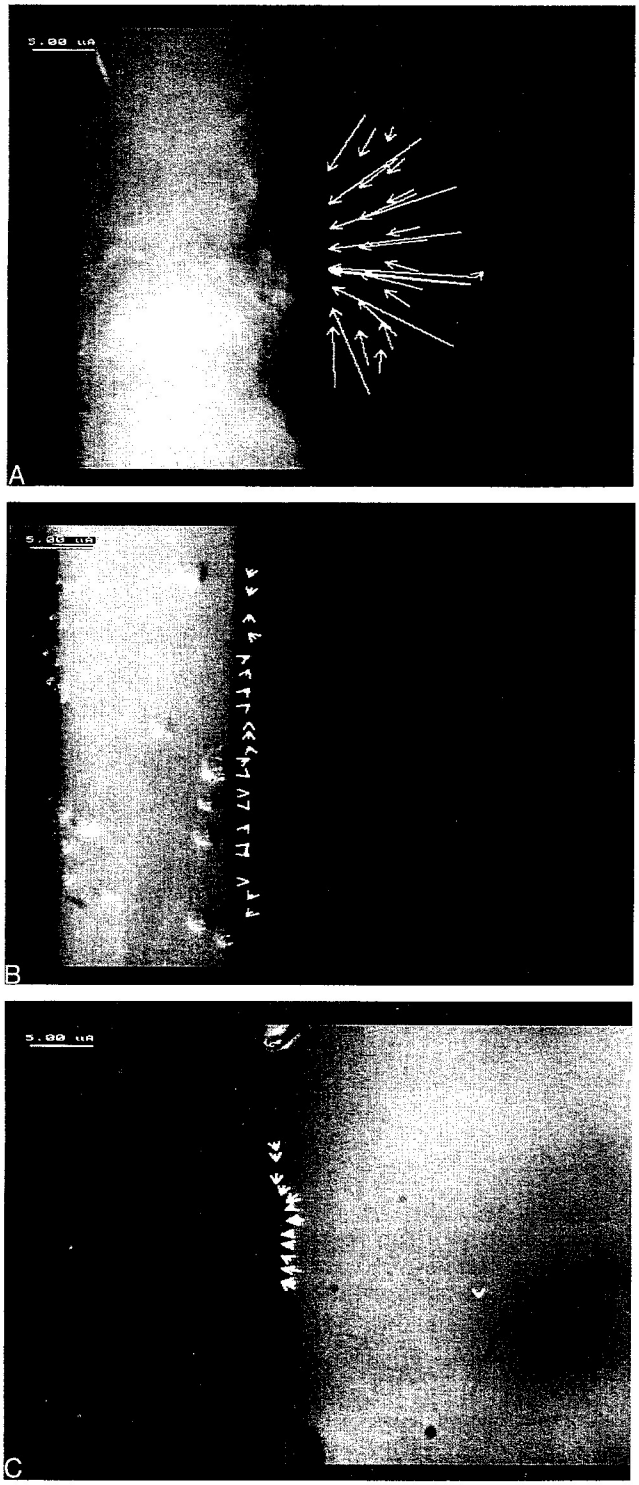

Fig. 2 (A) Damaged diaphysis of a living mouse metatarsal bone. The current density vectors are overlaid on the image. The bone damage is clearly visible as a round-shaped hole at the diaphyseal cortex. Each vector is created by the data acquisition and software conversion system and represents density (scale on top left), direction, and sign of the current measured at the point corresponding to the arrowhead. In this sample, several different recording positions were considered. Maximal current density was recorded over the center of the hole as shown by the position of longest vector entering the site of damage. The density of the current gradually decreased to background level as the probe was moved far from the center of the hole and far from the bone surface. The background level (<0.5 $\mu A/cm^2$) is represented here by an arrowhead which can only be seen far from the bone partly superimposed by the longest vector. **(B)** Intact diaphysis of a living bone (background level <0.5 $\mu A/cm^2$). **(C)** Damaged diaphysis of a dead bone (background level <0.5 $\mu A/cm^2$).

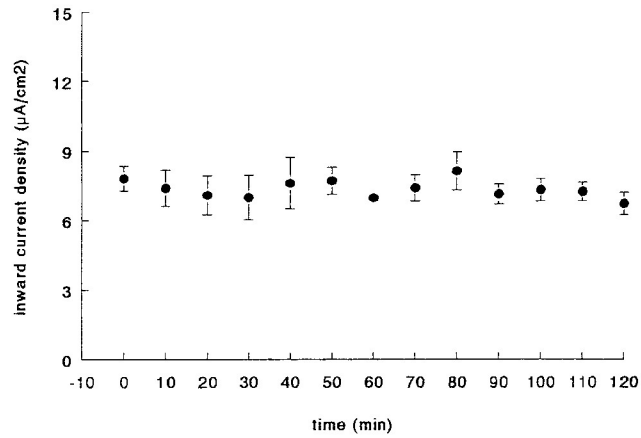

Fig. 3. Mean current density (bars indicate SEM) in bones (n = 3) incubated in sulfate medium. Current density was continuously monitored for 2 hours.

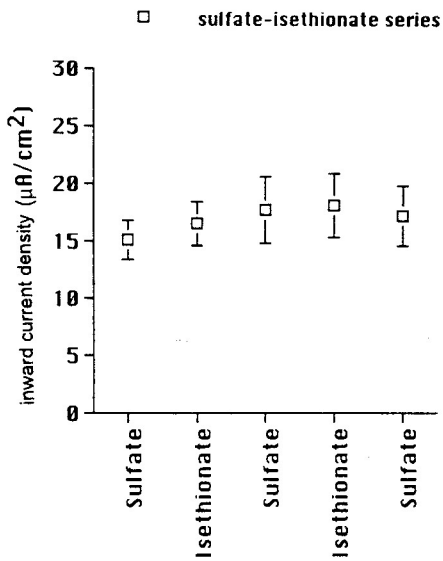

Fig. 4. Mean current density (bars indicate SEM) in bones (n = 7) alternately incubated in sulfate and isethionate media. The whole experiment lasted 80 minutes.

the endosteal surface, as suggested by the observation that ion currents occurred only when the hole was deep enough to reach the marrow cavity [1, 17]. Perhaps ion partitioning between bone and plasma [26] is exerted by bone-lining cells at the endosteal surface [27] and/or by epithelial-like squamous cells at the bone-marrow interface [28].

Role of Bicarbonate in Ionic Current

When bones are exposed to bicarbonate, the current density

Table 2. Actual pH and pCO_2 (mmHg), and calculated concentrations of HCO_3^- (mM) and total CO_2 (mM) when bones (n = 11) were incubated in bicarbonate medium

	Early bicarbonate					Late bicarbonate				
	pH	pO_2	pCO_2	HCO_3^-	tot CO_2	pH	pO_2	pCO_2	HCO_3^-	tot CO_2
Mean	7.35	136	63.8	33.7	35.6	7.37	138	63.3	34.9	36.8
SD	0.05	17	7.5	3.7	3.9	0.05	9	8.0	1.3	1.4

Early and late bicarbonate refer, respectively, to the first useful measurement after refoiling the chamber with bicarbonate, and the measurement taken 35 minutes later.

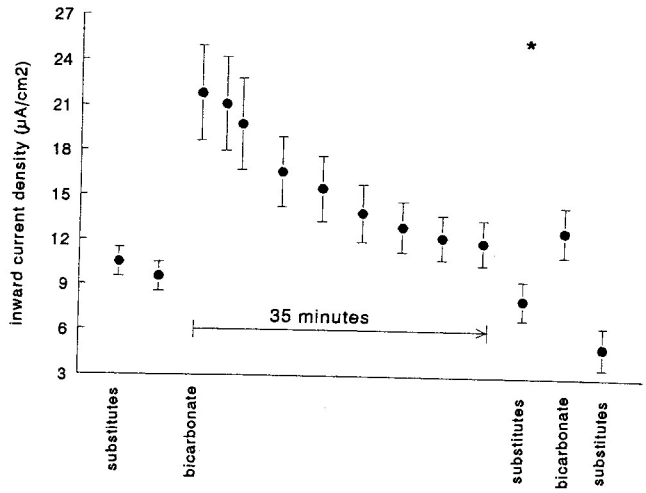

Fig. 5. Mean current density (bars indicate SEM) in bones incubated in sulfate or isethionate media and exposed to bicarbonate. Time scale is limited to the bicarbonate exposure. The whole experiment lasted 2 hours. The pattern of the decay refers to 10 of 12 bones. See text for detailed description. * = outlier not included in the analysis.

increases sharply then decays over the subsequent 35 minutes. These effects are theoretically associated with both the gas tightness of the system and the buffering power of the medium. In fact, bicarbonate participates to the equilibrium reaction $CO_2 + H_2O \Leftrightarrow H^+ + HCO_3^-$, where one component ($CO_2$) is volatile and the concentration of HCO_3^- is proportional to that of H^+. The rationale for the peculiar design of the experimental chamber, the use of mineral oil, and the almost-closed perfusing system is aimed at reducing to a reasonable minimum the exchange of CO_2 between the incubation medium and the atmosphere. Table 2 indicates that the selected experimental setup is suitable for the study described here where the total elapsed time for the measurements obtained in bone incubated in bicarbonate medium does not exceed 35 minutes. Furthermore, 10 mM HEPES buffer minimizes pH alterations. Therefore,we can reasonably exclude any specific changes of current density secondary to pH alterations or CO_2 leaks. The observed phenomena are linked to the presence of HCO_3^-.

The current density decayed in 10 out of 12 bones following a first-order exponential pattern. Thus, it is likely that a single factor, rather than a combination of multiple ones, is responsible for the decay. Possibly, hydration of bone bicarbonate pool by bone carbonic anhydrase [29] may account for the decay, but unfortunately we do not presently have data to support this hypothesis. Lack of early bicarbonate effects in two bones may be explained by the time delay between buffer exchange and the first useful measurement.

Skeletal carbon dioxide stores exist in two distinct forms: a stable one, that requires mineral and organic matrix dissolution for its availability [4] and a labile one, that is bicarbonate [3]. Our study supports the hypothesis that bicarbonate is exchanged with the extracellular ion compartment when bone CO_2 is lost to buffer blood pH during acute metabolic acidosis [26]. Since the bicarbonate store present in bone is large [3, 29] and the extension of the bone-plasma interface (1000–5000 m^2) is wider than lung capillary surfaces (140 m^2) [30], the physiological relevance of such exchange should be acknowledged.

In conclusion, damaged bones drive a steady ionic current through the site of damage. The current is probably related to the healing process and is originated by pump leak mechanisms at the bone-plasma interface. The net current results from a complex, not yet characterized ion exchange system, but HCO_3^- is clearly transported between bone and the surrounding medium. This confirms a major role for bone bicarbonate in short-term regulation of blood acid-base equilibrium and confirms the presence of an intense ion traffic between bone and plasma. Noteworthy is the fact that the characterization of this traffic is still lacking despite its discovery 20–30 years ago [31], but appropriate use of a two-dimensional vibrating probe system may represent an adequate tool to achieve this objective.

Acknowledgments. This work is dedicated to the memory of Luigi Divieti, Professor of Bioengineering, Politecnico of Milano. The authors are grateful to Carl Scheffey for the critical revision of the manuscript. This work was supported by grants from N.I.H., U.S.A. (RR01395), and CNR, Italy, Progetto Finalizzato Invecchiamento, n° INV 933375.

References

1. Borgens RB (1984) Endogenous ion currents traverse intact and damaged bone. Science 225:478–482
2. Jaffe LF, Nuccitelli R (1974) An ultrasensitive vibrating probe for measuring steady extracellular currents. J Cell Biol 63: 614–627
3. Poyart CF, Bursaux E, Freminet A (1975) The bone CO_2 compartment: evidence for a bicarbonate pool. Resp Physiol 25:89–99
4. Bettice JA (1984) Skeletal carbon dioxide stores during metabolic acidosis. Am J Physiol 247:F326–F330
5. Jennings ML (1992) Cellular anion transport. In: Seldin DW, Giebish G (eds) The kidney, physiology and pathophysiology. Raven Press, New York, pp 113–145
6. Scheffey C (1988) Two approaches to construction of vibrating probes for electrical current measurement in solution. Rev Sci Instrum 59:787–792
7. Biggers JD, Gwatkin RBL, Heyner S (1961) Growth of embrion avuan and mammalian tibiae on a relatively simple chemically defined medium. Exp Cell Res 25:41–58

8. Stern PH, Raisz LG (1979) Organ culture of bone. In: Skeletal research, Academic Press Inc., New York, pp 21–59
9. Scheffey C, Shipley AM, Durham JH (1991) Localization and regulation of acid-base secretory currents from individual epithelial cells. Am J Physiol 261:F963–974
10. Scheffey C (1986) Pitfalls of the vibrating probe technique and what to do about them. Prog Clin Biol Res 210:3–12
11. Ferrier J, Lucas WJ (1986) Ion transport and the vibrating probe. Biophys J 49:801–807
12. Nuccitelli R (1992) Endogenous ion currents and DC electric fields in multicellular animal tissues. Bioelectromagnetics (suppl 1):147–157
13. Betz WJ, Caldwell JA (1984) Mapping electric currents around skeletal muscle with a vibrating probe. J Gen Physiol 83:143–156
14. Friedenberg ZB, Brighton CT (1966) Bioelectric potentials in bone. J Bone Joint Surg 48A:915–923
15. Friedenberg ZB, Harlow MC, Heppenstall RB, Brighton CT (1973) The cellular origin of bioelectric potentials in bone. Calcif Tissue Res 13:53–62
16. Rubinacci A, Brigatti L, Tessari L (1984) A reference curve for axial bioelectric potentials in adult rabbit tibia. J Bioelectromagnetics 5:193–202
17. Chakkalakal DA, Wilson RF, Connolly JF (1988) Epidermal and endosteal sources of endogenous electricity in injured canine limbs. IEEE Trans Biom Eng 35:19–29
18. Jaffe L (1979) Control of development by ion currents. In: Cone RA, Dowling JE (eds) Membrane transduction mechanisms. Raven Press, New York, pp 199–231
19. Wirth DJ, Heidegger WJ, Beach KW (1986) Calcium homeostasis II: the sodium-potassium pump. Calcif Tissue Int 38: 306–307
20. McGrath KJ, Heideger WJ, Beach KW (1986) Calcium homeostasis III: the bone membrane potential and mineral dissolution. Calcif Tissue Int 39:279–283
21. Bushinsky DA, Chabala JM, Levi-Setti R (1989) Ion microprobe analysis of mouse calvariae in vitro: evidence for a "bone membrane." Am J Physiol 256:E152–E158
22. McCarthy ID, Hughes SPF (1990) Is there a blood-bone barrier? In: Arlet J, Mazieres B (eds) Springer, Berlin, pp 30–33
23. Trumbore DC, Heideger WJ, Beach KW (1980) Electrical potential difference across bone membrane. Calcif Tissue Int 32:159–168
24. Peterson DR, Heideger WJ, Beach KW (1985) Calcium homeostasis: the effect of parathyroid hormone on bone membrane electrical potential difference. Calcif Tissue Int 37: 307–311
25. Neumann WF, Ramp WK (1971) The concept of a bone membrane: some implications. In: Nichols G Jr, Wasserman RH (eds) Cellular mechanisms for calcium transfer and homeostasis. Academic Press, New York, pp 197–206
26. Green J, Kleeman CR (1991) Role of bone in regulation of systemic acid-base balance. Kidney Int 39:9–26
27. Miller SC, Bowman BM, Smith JM, Webster SS (1980) Characterization of endosteal bone-lining cells from fatty marrow bone sites in adult beagles. Anat Rec 198:163–173
28. Menton DN, Simmons DJ, Orr BY, Plurad SB (1982) A cellular investment of bone marrow. Anat Rec 203:157–164
29. Posner AS (1969) Crystal chemistry of bone mineral. Physiol Rev 49:760-792
30. Baron R (1993) Anatomy and ultrastructure of bone. In: Favus MJ (ed) Primer of the metabolic bone diseases and disorders of mineral metabolism. Raven Press, New York, p 3–9
31. Mundy GR (1989) Calcium homeostasis: hypercalcemia and hypocalcemia. Dunitz, London